Petrophysics of Magnetic Dipole Fields in an Anisotropic Earth

Allen Q. Howard, Jr, *Fellow, IEEE*

***Abstract*—Measurement-while-drilling (MWD) resistivity log data are often acquired in highly deviated or horizontal holes. The loop sensors are located on the drill collar and are approximated as magnetic dipoles. The conductivity of the earth in the vertical direction σ_v and horizontal direction σ_h are almost always different. When an MWD resistivity tool enters a new bed, the response is compared with the precomputed logs to aid in the determination of the location of the drill bit. The MWD tool response, however, is sensitive to resistivity anisotropy. An alternative method is used to derive analytical expressions for the Sommerfeld-type integrals. Numerical results give typical MWD tool response as a function of the inclination angle θ the tool makes with respect to the axes of anisotropy and also as a function of the anisotropy index $\kappa = (\sigma_h/\sigma_v)^{1/2}$.**

***Index Terms*—Apparent resistivity interpretation, electrical anisotropy, measurement-while-drilling (MWD) resistivity logging, Sommerfeld integrals, water saturation.**

I. Introduction

MEASUREMENT-while-drilling (MWD) resistivity log data is acquired as the hole is drilled. Modern drilling practice often positions the bore-hole horizontally in the oil bearing formation. The earth conductivity in the vertical direction σ_v and horizontal direction σ_h are almost always different. With the more mature technology of wireline logging, the loop sources are in more nearly vertical boreholes, where only the horizontal component σ_h is measured. It can be shown that the galvanic resistivity in the same environment measured by laterologs [1] also essentially measures $R_h = 1/\sigma_h$.

When an MWD resistivity tool enters a new bed, the response can be compared with precomputed logs to aid in the determination of the location of the drill bit. Therefore, comparison of wireline logs in vertical holes, with nearby MWD highly deviated holes is important. The MWD tool response, if in a more deviated hole, is sensitive to the resistivity anisotropy.

A paper on the effects of formation anisotropy on resistivity logs by Moran and Gianzero [2] is classic. The book by Wait [3] covers some of the same material in a more direct fashion. Recently, Hagiwara has published several papers on the interpretation of wireline and MWD logs in anisotropic layered media (an example containing other references is [4]).

The earth's conductivity may be anisotropic because in sedimentary rocks gravity differentiates the direction normal to the earth's surface. Sedimentary sequences under vertical stress produce as a consequence pore space geometries and often vertical fractures that differentiate horizontal and vertical permeability.

Klein and Allen [5] develop an interpretation of thinly laminated oil-saturated pay zones. Considered as a bulk medium, such zones are anisotropic. In particular, water wet oil-saturated formations with large variability in grain size can be highly anisotropic. Thus, significant anisotropy in porous sediments may be an indicator of hydrocarbon.

Manuscript received August 11, 1999; revised April 5, 2000. This work was supported by the Laboratório de Engenharia de Exploraço de Petróleo (LENEP), Universidade Estadual do Norte Fluminense (UENF), Macaé/RJ-Brasil.

The author is with the Department of Physics, Utah State University, Logan, UT 84322 USA (e-mail: terragraf@aol.com).

Publisher Item Identifier S 0018-926X(00)09345-5.

II. Theory

A common model for the earth's conductivity and dielectric anisotropy assumes that the vertical and horizontal components of conductivity are different. In this case, the conductivity dependence in Maxwell's equations enters as the tensor

$$\hat{\sigma} = \begin{bmatrix} \tilde{\sigma}_h & 0 & 0 \\ 0 & \tilde{\sigma}_h & 0 \\ 0 & 0 & \tilde{\sigma}_v \end{bmatrix} \tag{1}$$

where $\tilde{\sigma}_h = \sigma_h - i\omega\epsilon_h$ is the complex conductivity in the horizontal direction and a similar definition applies to the complex vertical conductivity $\tilde{\sigma}_v$. For a magnetic dipole source density $\mathbf{M}$ and a time dependence $e^{-i\omega t}$, Maxwell's equations in SI units [6] for anisotropic conductivity take the form

$$\begin{aligned} \nabla \times \mathbf{H}(\mathbf{x}) &= \hat{\sigma}\mathbf{E}(\mathbf{x}), \\ \nabla \times \mathbf{E}(\mathbf{x}) &= i\omega\mu_0[\mathbf{H}(\mathbf{x}) + \mathbf{M}(\mathbf{x})]. \end{aligned} \tag{2}$$

In (2), the earth's magnetic permeability is constant, isotropic, and equal to the vacuum value $\mu_0 = 4\pi \times 10^{-7}$ H/m. Because of conservation of total current $\nabla \cdot (\hat{\sigma}\mathbf{E}(\mathbf{x})) = 0$ and the vector identity $\nabla \cdot \nabla \times \mathbf{A}(\mathbf{x}) = 0$ for any vector field $\mathbf{A}(\mathbf{x})$, it follows that

$$\hat{\sigma}\mathbf{E}(\mathbf{x}) = k_h^2 \nabla \times \mathbf{\Pi}(\mathbf{x}) \tag{3}$$

where the Hertz vector $\mathbf{\Pi}(\mathbf{x})$ is yet to be determined, and the horizontal and vertical wavenumbers k_h and k_v are given by

$$\begin{aligned} k_h &= (i\omega\mu_0\tilde{\sigma}_h)^{1/2} \\ k_v &= (i\omega\mu_0\tilde{\sigma}_v)^{1/2}. \end{aligned} \tag{4}$$

The branch cut of the wave numbers in (4) is chosen such that $\mathrm{Im}(k_h) > 0, \mathrm{Im}(k_v) > 0$. Substitution of (3) into Ampere's law, i.e., the first equation of (2) defines the magnetic intensity $\mathbf{H}(\mathbf{x})$ as

$$\mathbf{H}(\mathbf{x}) = k_h^2 \mathbf{\Pi}(\mathbf{x}) + \nabla\Phi(\mathbf{x}) \tag{5}$$

for any scalar potential $\mathbf{\Phi}(\mathbf{x})$. Because (3) only defines the curl of the vector potential $\mathbf{\Pi}(\mathbf{x})$, it is possible to invoke the gauge condition

$$\nabla \cdot \hat{\sigma}\mathbf{\Pi}(\mathbf{x}) = \tilde{\sigma}_v \mathbf{\Phi}(\mathbf{x}). \tag{6}$$

From (3), it follows that

$$\mathbf{E}(\mathbf{x}) = i\omega\mu_0 \begin{bmatrix} 1 & 0 & 0 \\ 0 & 1 & 0 \\ 0 & 0 & \kappa^2 \end{bmatrix} \nabla \times \mathbf{\Pi}(\mathbf{x}) \tag{7}$$

where the anisotropic index κ is given by

$$\kappa = \left(\frac{\tilde{\sigma}_h}{\tilde{\sigma}_v}\right)^{1/2}. \tag{8}$$

Similarly, the magnetic intensity $\mathbf{H}(\mathbf{x})$ from (5) and (6) is defined as

$$\mathbf{H}(\mathbf{x}) = k_h^2 \mathbf{\Pi}(\mathbf{x}) + \nabla\nabla \cdot \begin{bmatrix} \kappa^2 & 0 & 0 \\ 0 & \kappa^2 & 0 \\ 0 & 0 & 1 \end{bmatrix} \mathbf{\Pi}(\mathbf{x}). \tag{9}$$

Now substitute (7) and (9) into Faraday's law defined by the second of (2). After simplification, the three Cartesian component equations for the determination of the Hertz potential $\mathbf{\Pi}(\mathbf{x})$ are found to be

$$\begin{aligned} \nabla_t^2 \Pi_x + \frac{1}{\kappa^2}\partial_z^2 \Pi_x + k_v^2 \Pi_x &= -M_x/\kappa^2, \\ \nabla_t^2 \Pi_y + \frac{1}{\kappa^2}\partial_z^2 \Pi_y + k_v^2 \Pi_y &= -M_y/\kappa^2 \\ \nabla^2 \Pi_z + k_h^2 \Pi_z &= -M_z + (1+\kappa^2) \\ &\quad \cdot \partial_z[\partial_x \Pi_x + \partial_y \Pi_y]. \end{aligned} \tag{10}$$

In (10), $\nabla_t^2 = \partial_x^2 + \partial_y^2$, and $\nabla^2 = \nabla_t^2 + \partial_z^2$ is the usual Laplacian operator in Cartesian coordinates. The next section gives a solution of (10).

III. Homogeneous Medium Solution

The x and y components of (10), except for a rescaling of the z axis have a simple solution, i.e., let

$$\mathcal{Z} = \kappa z \tag{11}$$

then (10) for Π_x is

$$\hat{\nabla}^2 \Pi_x + k_v^2 \Pi_x = -\frac{M_x}{\kappa^2} \tag{12}$$

where $\hat{\nabla}^2 = \partial_x^2 + \partial_y^2 + \partial_{\mathcal{Z}}^2$. For point magnetic dipoles

$$M_x = m_x \delta^{(3)}(\mathbf{x} - \mathbf{x}_T) \tag{13}$$

and similarly for M_y and M_z, where $\delta^{(3)}(\mathbf{x} - \mathbf{x}_T)$ is the three-dimensional (3-D) Dirac delta function and $m_x = I_0\, dA$ for a small loop of area dA and current I_0. For point source dipoles then

$$\begin{aligned} \Pi_x(\mathbf{x}) &= \frac{m_x}{4\pi\kappa^2} \frac{e^{ik_v \tilde{R}}}{\tilde{R}} \\ \Pi_y(\mathbf{x}) &= \frac{m_y}{4\pi\kappa^2} \frac{e^{ik_v \tilde{R}}}{\tilde{R}} \end{aligned} \tag{14}$$

where $\tilde{R} = ((x-x_T)^2 + (y-y_T)^2 + \kappa^2(z-z_T)^2)^{1/2}$, and $\mathbf{x}_T$ is the location of the magnetic dipole source.

To model a resistivity log traversing an anisotropic medium at an angle θ with respect to the vertical z axis (the direction associated with σ_v), it is sufficient to consider two problems. One with source M_z only, the other with source M_x. A linear combination of these solutions gives the solution at an inclination angle θ. In the following, the tool axis is in the plane $y = 0$.

The M_z source problem is elementary, but the M_x source for Π_z is more difficult because of the coupling term involving Π_x and Π_y. In the literature ([2] and [3]), the approach uses Fourier–Bessel transforms to reduce the third (10) to an ordinary differential equation. Then a homogenous solution is added to the particular solution such that in the limit as κ approaches one, the potential Π_z vanishes if $M_z = 0$. The problem with this is that there are many homogeneous solutions with this property, each with different factors of κ having a common limit when κ approaches one. Thus, such solutions are not unique.

To insure uniqueness, note that from (10c) for Π_z, when $\mathbf{M} = (M_x, 0, 0)$, the formal solution Π_{z2} via potential theory is

$$\Pi_{z2}(\mathbf{x}) = (\kappa^2 - 1)\partial_{zx}^2 \int g_0(\mathbf{x}, \mathbf{x}')\Pi_x(\mathbf{x}')\, d^3x' \tag{15}$$

where

$$g_0(\mathbf{x}, \mathbf{x}') = \frac{e^{ik_h R}}{4\pi R}, \quad R = |\mathbf{x} - \mathbf{x}'|. \tag{16}$$

The integral on the right-hand side of (15) is a 3-D convolution, so that by the convolution theorem, Π_{z2} has the alternative representation

$$\Pi_{z2}(\mathbf{x}) = (\kappa^2 - 1)\partial_{zx}^2 \int e^{i\mathbf{K}\cdot\mathbf{x}} G_0(\mathbf{K})\Pi_x(\mathbf{K}) \frac{d^3K}{(2\pi)^3} \tag{17}$$

where the spectral form G_0 is

$$G_0(\mathbf{K}) = \frac{1}{K_z^2 - k_{zh}^2}. \tag{18}$$

Compare (14) and (16) and note the transform of (16) is (18). This leads to the representation

$$\Pi_x(\mathbf{K}) = \frac{m_x}{\kappa} \frac{e^{-i\mathbf{K}\cdot\mathbf{x}_T}}{K_z^2 - k_{zv}^2} \tag{19}$$

where $\mathbf{x}_T$ is the magnetic dipole location and in (17)–(19) the wave number notation is

$$\begin{aligned} \mathbf{K} &= K_x \mathbf{i}_x + K_y \mathbf{i}_y + K_z \mathbf{i}_z \\ \mathbf{K}\cdot\mathbf{x} &= K_x x + K_y y + K_z z \\ d^3K &= dK_x\, dK_y\, dK_z \\ k_{zh} &= (k_h^2 - \lambda^2)^{1/2}, \quad \mathrm{Im}(k_{zh}) > 0 \\ k_{zv} &= (k_h^2 - \kappa^2\lambda^2)^{1/2}, \quad \mathrm{Im}(k_{zv}) > 0 \\ \lambda^2 &= K_x^2 + K_y^2. \end{aligned} \tag{20}$$

Substitute representations (19) and (18) into (17) to obtain

$$\Pi_{z2}(\mathbf{x}) = \frac{m_x}{\kappa}(\kappa^2 - 1)\partial_{zx}^2 I_z(\mathbf{x}) \tag{21}$$

where

$$I_z(\mathbf{x}) = \int \frac{e^{i\mathbf{K}\cdot(\mathbf{x}-\mathbf{x}_T)}}{(K_z^2 - k_{zh}^2)(K_z^2 - k_{zv}^2)} \frac{d^3K}{(2\pi)^3}. \quad (22)$$

In cylindrical coordinates, the wave number elemental volume in (22) is $d^3K = \lambda\, d\lambda\, d\phi_K\, dK_z$. The K_z integration in (22) is a residue calculation resulting in

$$\int_{-\infty}^{\infty} \frac{e^{iK_z(z-z_T)}}{(K_z^2 - k_{zh}^2)(K_z^2 - k_{zv}^2)}\, dK_z = \frac{\pi i}{(\kappa^2-1)\lambda^2}\left[\frac{e^{ik_{zh}|z-z_T|}}{k_{zh}} - \frac{e^{ik_{zv}|z-z_T|}}{k_{zv}}\right]. \quad (23)$$

The angle integration is

$$\int_0^{2\pi} e^{i\mathbf{K}_t\cdot(\mathbf{x}-\mathbf{x}_T)}\, d\phi_k = 2\pi J_0(\lambda r) \quad (24)$$

where

$$\begin{aligned} r &= \left((x-x_T)^2 + (y-y_T)^2\right)^{1/2} \\ \mathbf{K}_t &= K_x\mathbf{i}_x + K_y\mathbf{i}_y \\ \lambda &= (K_x^2 + K_y^2)^{1/2}. \end{aligned} \quad (25)$$

Combining results (23) and (24) determines

$$\Pi_{z2}(\mathbf{x}) = \frac{m_x}{4\pi\kappa}\frac{\partial r}{\partial x}\int_0^{\infty} J_1(\lambda r) \cdot\left[e^{ik_{zh}|z-z_T|} - e^{ik_{zv}|z-z_T|}\right] d\lambda \quad (26)$$

Let the transmitter magnetic dipole be rotated about the y axis by an angle θ and without loss of generality, assume the tool is in the plane $y = 0$, with transmitter at the origin so that $\mathbf{x}_T = 0$. Then in (27), $\partial r/\partial x = \cos\phi = 1$, $r = |x|$, and the magnetic dipole density M is

$$M = m\sin\theta\,\mathbf{i}_x + m\cos\theta\,\mathbf{i}_z. \quad (27)$$

Thus, by superposition, the Hertz vector is

$$\mathbf{\Pi}(\mathbf{x}) = \Pi_x(\mathbf{x})\mathbf{i}_x + \Pi_z(\mathbf{x})\mathbf{i}_z \quad (28)$$

and from (9), the resulting magnetic intensity components are

$$\begin{aligned} H_x(\mathbf{x}) &= k_h^2\Pi_x(\mathbf{x}) + \kappa^2\partial_{xx}^2\Pi_x(\mathbf{x}) + \partial_{xz}^2\Pi_z(\mathbf{x}) \\ H_z(\mathbf{x}) &= k_h^2\Pi_z(\mathbf{x}) + \kappa^2\partial_{zx}^2\Pi_x(\mathbf{x}) + \partial_{zz}^2\Pi_z(\mathbf{x}). \end{aligned} \quad (29)$$

In (29)

$$\begin{aligned} \Pi_x(\mathbf{x}) &= \frac{m_x}{4\pi\kappa^2}\frac{e^{ik_v\tilde{R}}}{\tilde{R}} \\ \Pi_z(\mathbf{x}) &= \pi_{z1}(\mathbf{x}) + \pi_{z2}(\mathbf{x}) \\ \Pi_{z1}(\mathbf{x}) &= \frac{m_z}{4\pi}, \frac{e^{ik_h R}}{R} \\ \Pi_{z2}(\mathbf{x}) &= \frac{m_x}{4\pi\kappa}\int_0^{\infty} J_1(\lambda\rho) \cdot\left[e^{ik_{zh}|z-z_T|} - e^{ik_{zv}|z-z_T|}\right] d\lambda. \end{aligned} \quad (30)$$

Note as a check on the results, when $\kappa = 1$, $\Pi_{z2}(\mathbf{x}) = 0$, as it should. In the tool coordinate system, the axial magnetic intensity H_z' is thus

$$H_z'(\mathbf{x}) = \cos\theta\, H_z(\mathbf{x}) + \sin\theta\, H_x(\mathbf{x}). \quad (31)$$

The complex receiver voltage for a two-coil magnetic dipole sonde with an inclination angle θ in an anisotropic medium is thus

$$v(L,\,\theta,\,\kappa,\,\sigma_h) = i\omega\mu_0 m_R H_z'(\mathbf{x}_R) \quad (32)$$

where

$$\begin{aligned} \mathbf{x}_R &= L\sin\theta\,\mathbf{i}_x + L\cos\theta\,\mathbf{i}_z \\ m_R &= N_R A_R \end{aligned} \quad (33)$$

and N_R is the number of turns in the receiver coil with cross-sectional area A_R. In (33), L is the distance between transmitter and receiver coils. The Appendix contains numerical details for computing voltage v given by (33).

IV. Conductivity Tensor at an Oblique Angle

An oblique angle with respect to the anisotropy axis is common in MWD resistivity logs. In this case the tool axis in direction z, and the z' axis defining the direction of $\tilde{\sigma}_v$ form an angle θ. For a rotation of angle θ about the y axis (i.e. such that $y = y'$), we have

$$\begin{bmatrix} x' \\ y' \\ z' \end{bmatrix} = R(\theta)\begin{bmatrix} x \\ y \\ z \end{bmatrix} \quad (34)$$

where the rotation matrix $R(\theta)$ is defined as

$$R(\theta) = \begin{bmatrix} \cos\theta & 0 & -\sin\theta \\ 0 & 1 & 0 \\ \sin\theta & 0 & \cos\theta \end{bmatrix}. \quad (35)$$

We can use the rotation matrix $R(\theta)$ defined by (35) to determine the effective anisotropy matrix $\hat{\sigma}$ in the tool coordinate system as follows. Ohm's law applies equally in either coordinate system, i.e.,

$$\begin{aligned} \mathbf{J} &= \hat{\sigma}\mathbf{E} \\ \mathbf{J}' &= \hat{\sigma}'\mathbf{E}'. \end{aligned} \quad (36)$$

In the primed axis, the conductivity anisotropy tensor $\hat{\sigma}'$ is defined by (1). To determine the form of the anisotropy tensor $\hat{\sigma}$ in the tool coordinate system, note that the vector fields obey the same transform law as the coordinate vectors in (34). Thus,

$$\begin{aligned} \mathbf{J}' &= R(\theta)\mathbf{J} \\ \mathbf{E}' &= R(\theta)\mathbf{E}. \end{aligned} \quad (37)$$

It follows from (36) and (37) that

$$\hat{\sigma} = R^{-1}(\theta)\hat{\sigma}'R(\theta). \quad (38)$$

Rotation matrices are special in the sense that

$$R^{-1}(\theta) = R(-\theta) = \begin{bmatrix} \cos\theta & 0 & \sin\theta \\ 0 & 1 & 0 \\ -\sin\theta & 0 & \cos\theta \end{bmatrix}. \quad (39)$$

Thus, from (38) and (39), the tool coordinate system anisotropy tensor $\hat{\sigma}$ is

$$\hat{\sigma} = \begin{bmatrix} \cos^2\theta\hat{\sigma}_h + \sin^2\theta_v & 0 & \sin\theta\cos\theta(\tilde{\sigma}_v - \tilde{\sigma}_h) \\ 0 & \tilde{\sigma}_h & 0 \\ \sin\theta\cos\theta(\tilde{\sigma}_v - \tilde{\sigma}_h) & 0 & \sin^2\theta\tilde{\sigma}_h + \cos^2\theta\tilde{\sigma}_v \end{bmatrix}. \quad (40)$$

As a check, note that $\lim_{\theta\to 0}\hat{\sigma} = \hat{\sigma}'$.

V. Linearized Apparent Resistivity

In the tool system of coordinates, with tool axis inclined at an angle θ with respect to the z axis of the anisotropy, the conductivity tensor is given by (40). This tensor enables us to determine the apparent resistivity for borehole with inclination angle θ in an anisotropic medium. The transmitter loop induces an azimuthal current component J_ϕ in the formation. Now

$$\begin{bmatrix} J_x \\ J_y \end{bmatrix} = \begin{bmatrix} \cos\phi & -\sin\phi \\ \sin\phi & \cos\phi \end{bmatrix} \begin{bmatrix} J_\rho \\ J_\phi \end{bmatrix} \quad (41)$$

and similarly

$$\begin{bmatrix} E_x \\ E_y \end{bmatrix} = \begin{bmatrix} \cos\phi & -\sin\phi \\ \sin\phi & \cos\phi \end{bmatrix} \begin{bmatrix} E_\rho \\ E_\phi \end{bmatrix}. \quad (42)$$

In the tool coordinate system, Ohm's law is

$$\begin{bmatrix} J_x \\ J_y \end{bmatrix} = \begin{bmatrix} \tilde{\sigma}_{xx} & \tilde{\sigma}_{xy} \\ \tilde{\sigma}_{yx} & \tilde{\sigma}_{yy} \end{bmatrix} \begin{bmatrix} E_x \\ E_y \end{bmatrix}. \quad (43)$$

Substitution of (41) and (42) into (43) determines

$$\begin{bmatrix} J_\rho \\ J_\phi \end{bmatrix} = \begin{bmatrix} \sigma_{11} & \sigma_{12} \\ \sigma_{21} & \sigma_{22} \end{bmatrix} \begin{bmatrix} E_\rho \\ E_\phi \end{bmatrix} \quad (44)$$

where from (40)

$$\begin{aligned} \sigma_{11} &= \cos^2\phi\tilde{\sigma}_{xx} + \sin^2\phi\tilde{\sigma}_{yy} \\ \sigma_{12} &= \sin\phi\cos\phi(\tilde{\sigma}_{yy} - \tilde{\sigma}_{xx}) \\ \sigma_{21} &= \sin\phi\cos\phi(\tilde{\sigma}_{yy} - \tilde{\sigma}_{xx}) \\ \sigma_{22} &= \sin^2\phi\tilde{\sigma}_{xx} + \cos^2\phi\tilde{\sigma}_{yy} \end{aligned} \quad (45)$$

and where

$$\begin{aligned} \tilde{\sigma}_{xx} &= \cos^2\theta\,\tilde{\sigma}_h + \sin^2\theta\,\tilde{\sigma}_v \\ \tilde{\sigma}_{yy} &= \tilde{\sigma}_h. \end{aligned} \quad (46)$$

Equation (44) shows that the conductivity tensor is a function of the azimuthal angle ϕ. The resistivity measurement averages over ϕ. Taking the average value of the 2×2 conductivity tensor in (44) gives

$$\frac{1}{2\pi}\int_0^{2\pi} d\theta \begin{bmatrix} \sigma_{11} & \sigma_{12} \\ \sigma_{21} & \sigma_{22} \end{bmatrix} = \begin{bmatrix} \frac{1}{2}(\tilde{\sigma}_{xx} + \tilde{\sigma}_{yy}) & 0 \\ 0 & \frac{1}{2}(\tilde{\sigma}_{xx} + \tilde{\sigma}_{yy}) \end{bmatrix}. \quad (47)$$

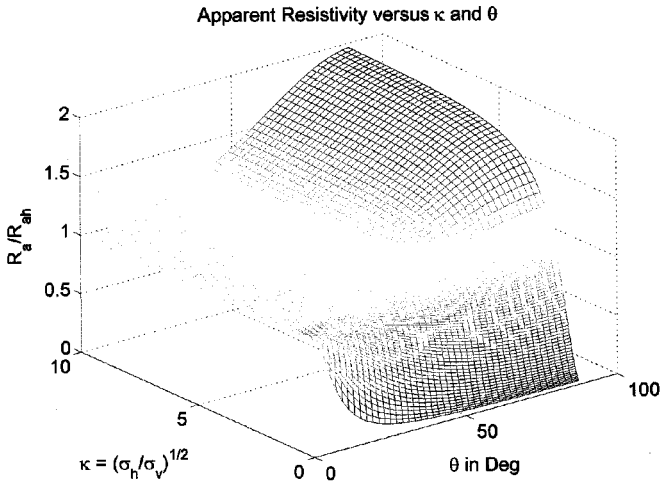

Fig. 1. Ratio R_a/R_h versus θ in degrees and anisotropic ratio κ.

Result (47) yields the azimuthally averaged formation conductivity $\langle\tilde{\sigma}_\phi\rangle$

$$\langle\tilde{\sigma}_\phi\rangle = \frac{\tilde{\sigma}_h}{2\kappa^2}\left(\sin^2\theta + \kappa^2(1+\cos^2\theta)\right). \quad (48)$$

Conductivity $\langle\tilde{\sigma}_\phi\rangle$ is an equivalent isotropic medium conductivity for given parameters θ and κ. By definition, the real part of the receiver voltage in a conductivity measuring tool is proportional to the apparent conductivity σ_a. The constant of proportionality, called the tool constant, is independent of formation conductivity. It depends only on tool parameter. Because of this, it follows from (48) that the linearized apparent resistivity R_a for an anisotropic medium is given by

$$R_a = \frac{R_{ah}2\kappa^2}{\sin^2\theta + \kappa^2(1+\cos^2\theta)} \quad (49)$$

where R_{ah} is the apparent resistivity in a homogenous isotropic conducting medium with resistivity $R_h = 1/\sigma_h$. Note the limiting value $\lim_{\theta\to 0} R_a = R_{ah}$. Note also this formula for R_a is different from Hagiwara's [4] and that of Moran and Gianzero [2]. Because details of the linearized R_a computation are not in [2] and [4], I cannot account for the differences. A more fundamental and complete MWD apparent resistivity in given the next section. Fig. 1 is a two-dimensional (2-D) plot of the ratio R_a/R_{ah} versus θ in degrees and anisotropic ratio κ.

VI. MWD Apparent Resistivity

MWD tools typically derive formation resistivity from ratios of received voltage from two adjacent receivers. Thus, consider one transmitter and two receivers spaced distances L_1 and L_2 from the transmitter along the tool axis. Then the voltage ratio $\mathcal{R}$ is

$$\mathcal{R} = v(L_1, \theta, \kappa, \sigma_h)/v(L_2, \theta, \kappa, \sigma_h). \quad (50)$$

This is a complex number with magnitude and phase angle. The ratio of measurements removes some of the sensitivity to the borehole environment and thus is an improvement over interpretation based upon a simple two-coil measurement.

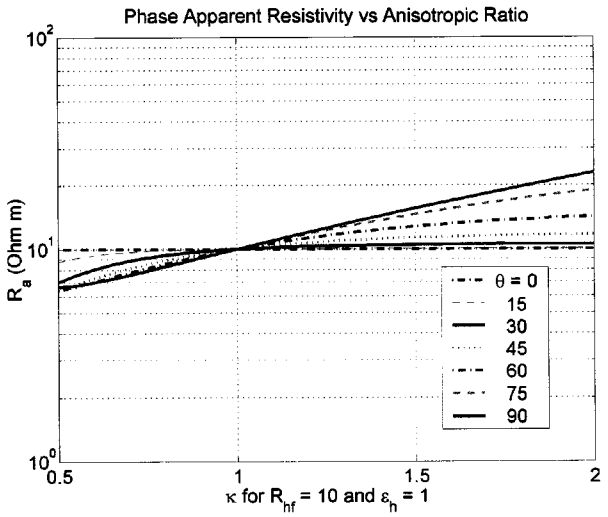

Fig. 2. Phase apparent resistivity R_{aph} defined by (57) for parameters in list (59).

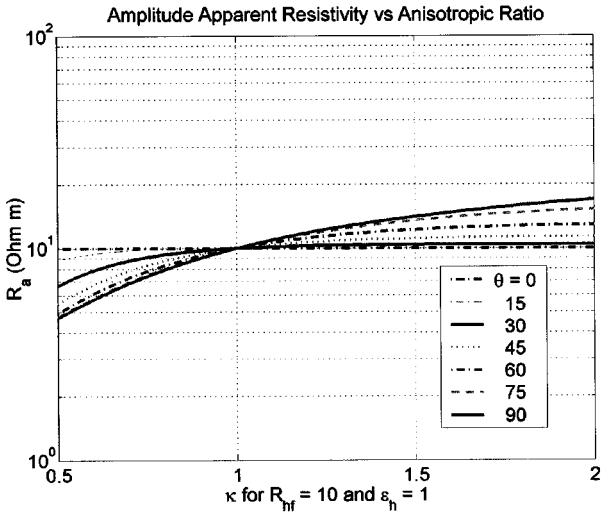

Fig. 3. Amplitude apparent resistivity R_{aph} defined by (57) for parameters in list (59).

For purposes of tool calibration, an MWD tool reading is taken in the air not near conductors. This results in the air-hang correction

$$\mathcal{R}_{ah} = v(L_1, \theta, \kappa, \mathbf{0})/v(L_2, \theta, \kappa, \mathbf{0}). \tag{51}$$

The air-hang corrected voltage ratio $\mathcal{R}_c$ is thus defined as

$$\mathcal{R}_c = \mathcal{R}/\mathcal{R}_{ah}. \tag{52}$$

Note $\mathcal{R}_c$ has unity magnitude and zero phase in the limit as σ_h tends to zero. In terms of phase and amplitude, i.e,

$$\begin{aligned} \phi &= \arg(\mathcal{R}_c), \quad \text{(in degrees)} \\ \mathrm{A_{dB}} &= 20\log_{10}|\mathcal{R}_c|, \quad \text{(in dB)} \end{aligned} \tag{53}$$

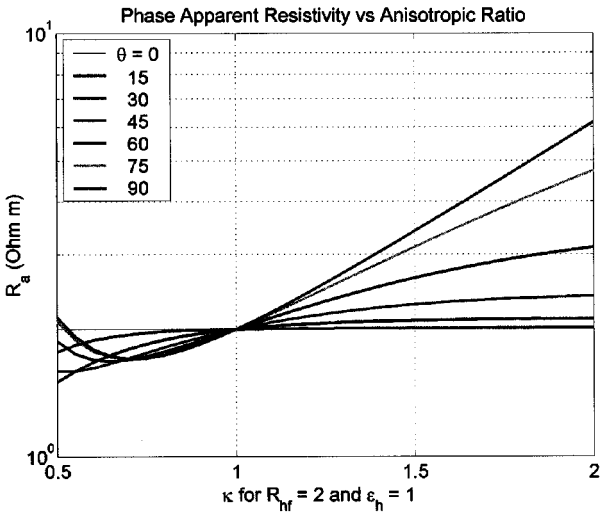

Fig. 4. Phase apparent resistivity R_{aph} defined by (57) for parameters in list (59).

the ratio $\mathcal{R}_c$ has a phase and amplitude apparent resistivity. To determine the equivalent apparent resistivities, compute a look up table of $\mathcal{R}_{c0}$ as a function of formation conductivity σ_h where

$$\mathcal{R}_{c0} = \mathcal{R}_0/\mathcal{R}_{ah}. \tag{54}$$

In (54), $\mathcal{R}_0$ is the equivalent homogeneous medium response

$$\mathcal{R}_0 = v(L_1, \theta, 1, \sigma_h)/v(L_2, \theta, 1, \sigma_h). \tag{55}$$

Define homogeneous phase and amplitude as

$$\begin{aligned} \phi_0 &= \arg(\mathcal{R}_{c0}), \quad \text{(in degrees)} \\ \mathrm{A_{dB0}} &= 20\log_{10}|\mathcal{R}_{c0}|, \quad \text{(in dB)}. \end{aligned} \tag{56}$$

Given tables of $[\phi_0, \sigma_h]$ and $[\mathrm{A_{dB0}}, \sigma_h]$, the apparent phase and amplitude resistivities R_{aph} and R_{aam} are determined by interpolation, i.e.,

$$\begin{aligned} R_{aph} &= 1/\mathrm{interp}(\phi_0, \sigma_h, \phi) \\ R_{aam} &= 1/\mathrm{interp}(\mathrm{A_{dB0}}, \sigma_h, \mathrm{A_{dB}}). \end{aligned} \tag{57}$$

In (57), the function *interp*, given a lookup table $[x, y]$, computes an interpolated ordinate y_i, given an index value x_i, i.e.,

$$y_i = \mathrm{interp}(x, y, x_i). \tag{58}$$

Because electromagnetic resistivity tools are sensitive to conductivity, interpolation is done in conductivity units and then converted to resistivity.

Experience with log interpretation and modeling of MWD resistivity supports the notion that the phase resistivity curve has a slightly more shallow depth of investigation than the corresponding amplitude curve. In a vertical well, separation of the two curves can be interpreted as invasion of borehole fluid into the formation.

For numerical results, use the following parameters:

$$\begin{aligned}
\epsilon_h &= 1.0, \\
L_1 &= 0.6350\ \text{m},\ (25\,\text{in}) \\
L_2 &= 0.7874\ \text{m},\ (31\,\text{in}) \\
\theta &= [0 : 15 : 90],\ \text{Degrees} \\
\kappa &= [0 : 5 : 0.05 : 2] \\
a_T &= 0.086\,360\ \text{m} \\
N_T &= 1\ \text{turns} \\
N_R &= 1\ \text{turns} \\
\mu &= \mu_0 = 4\pi\,10^{-7}\ \text{H/m} \\
f &= 2\ \text{MHz}.
\end{aligned} \tag{59}$$

For the air-hang correction, use $\sigma = 5.0 \times 10^{-4}$ S/m, and $\epsilon = 1.01$. Figs. 2–5 plot apparent resistivity R_a as defined by (57) versus the anisotropic ratio κ for seven inclination angles θ in degrees as displayed in the legend. Figs. 2 and 3 are, respectively, the phase and amplitude apparent resistivities for $\sigma_h = 0.1$ S/m. Similarly, Figs. 4 and 5 are, respectively, the phase and amplitude apparent resistivities for $\sigma_h = 0.5$ S/m. Note that in Figs. 2–5, for $\kappa = 1$, the medium is isotropic, and the family of θ curves cross the point $R_a = R_h$, as is necessary. In general, the apparent resistivity depends upon both κ and θ and the phase and amplitude apparent resistivities are not the same.

VII. Anisotropy of Thinly Laminated Formations

A long time ago, Conrad and Marcel Schlumberger showed [7] that fine laminations or sequences of shale and sand bedding give rise to an equivalent anisotropic medium when the bed thicknesses are small compared to the distance L between source and receiver loops of a conductivity sonde. Such layering is common in sedimentary reservoir rock. Let the volume fractions of shale and sand be v_{sh} and v_{sa}. In the case of horizontal resistivity, the resistivities add in parallel. Recall that resistance R in ohms is defined in terms of the bulk medium resistivity ρ as $R = \rho L/A$, where A is a cross-sectional area perpendicular to the direction of current flow, and L is the dimension of the bulk resistor in the direction of current flow. It follows that the bulk horizontal resistivity ρ_h is

$$\left(\frac{\rho_h}{v_{sh}+v_{sa}}\right)^{-1} = \left(\frac{\rho_{sh}}{v_{sh}}\right)^{-1} + \left(\frac{\rho_{sa}}{v_{sa}}\right)^{-1} \tag{60}$$

or

$$\rho_h = \rho_{sh}\rho_{sa}(v_{sh}+v_{sa})/(v_{sh}\rho_{sa}+v_{sa}\rho_{sh}). \tag{61}$$

Converting to conductivity gives

$$\sigma_h = (\sigma_{sh}v_{sh}+\sigma_{sa}v_{sa})/(v_{sh}+v_{sa}). \tag{62}$$

Similarly, vertical resistivity is computed as resistors in series, hence

$$\rho_v = (\rho_{sh}v_{sh}+\rho_{sa}v_{sa})/(v_{sh}+v_{sa}) \tag{63}$$

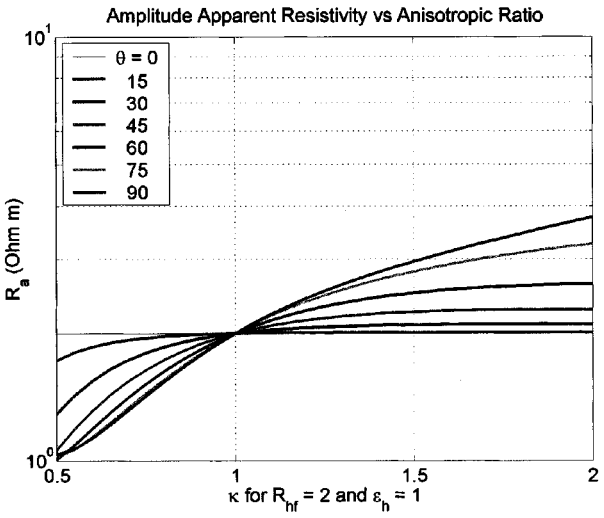

Fig. 5. Amplitude apparent resistivity R_{aph} defined by (57) for parameters in list (59).

or, in conductivity

$$\sigma_v = \sigma_{sh}\sigma_{sa}(v_{sh}+v_{sa})/(v_{sh}\sigma_{sa}+v_{sa}\sigma_{sh}). \tag{64}$$

The anisotropic ratio $\kappa^2 = \sigma_h/\sigma_v$ for this sandstone shale sequence is thus

$$\kappa^2 = \frac{(\sigma_{sh}v_{sh}+\sigma_{sa}v_{sa})(\sigma_{sa}v_{sh}+\sigma_{sh}v_{sa})}{(v_{sh}+v_{sa})^2\sigma_{sh}\sigma_{sa}} \tag{65}$$

or in more compact form

$$\kappa = [(\gamma V_{sh}+V_{sa})(V_{sh}/\gamma+V_{sa})]^{1/2} \tag{66}$$

where V_{sh} and V_{sa} are the relative shale and sand volumes

$$\begin{aligned}
V_{sh} &= \frac{v_{sh}}{v_{sh}+v_{sa}} \\
V_{sa} &= \frac{v_{sa}}{v_{sh}+v_{sa}} \\
\gamma &= \frac{\sigma_{sh}}{\sigma_{sa}}.
\end{aligned} \tag{67}$$

Fig. 6 is a 2-D plot of the anisotropic index κ versus the ratio $\gamma = \sigma_{sh}/\sigma_{sa}$ and the fractional shale volume V_{sh}.

VIII. Anisotropy of Laminated Formations as a Function of Water Saturation S_w

Klein *et al.* in [5] demonstrates the sensitivity of the anisotropic index κ on the effective water saturation S_w of finely laminated sequences. They use pore-space capillary pressure as a parameter to relate the water saturation of shale (S_{wsh}) and water saturation of the sandstone member (S_{wsa}). To study this effect, use (66), but where now γ is defined as a function of water saturation, i.e.,

$$\gamma = \frac{(S_{wsh}\phi_{sh})^2}{(S_{wsa}\phi_{sa})^2}. \tag{68}$$

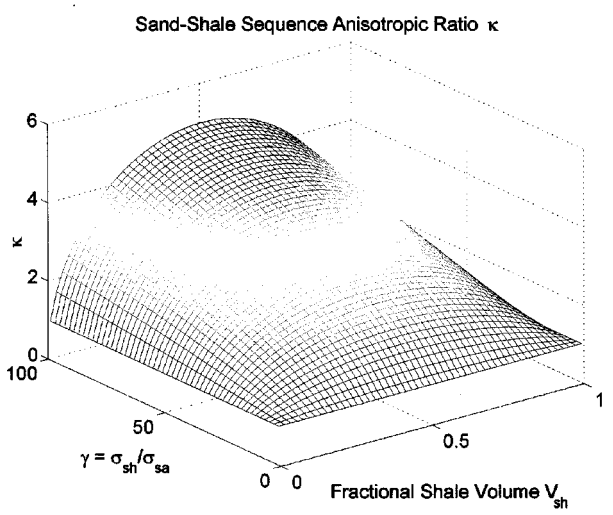

Fig. 6. Anisotropy ratio κ versus fractional shale volume V_{sh} and shale to sandstone conductivity ratio γ.

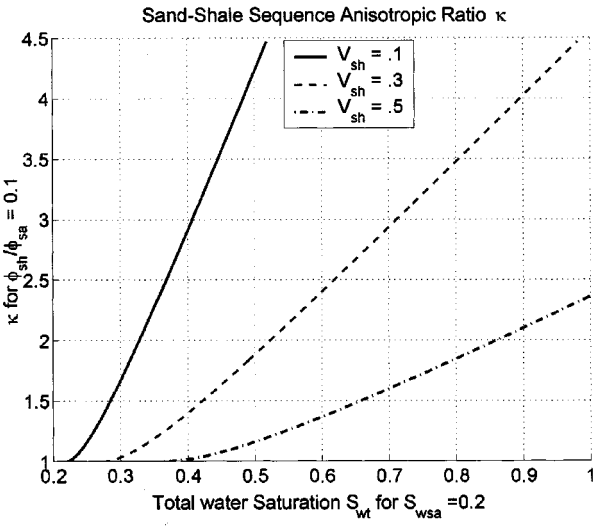

Fig. 7. Anisotropy ratio κ versus total water saturation S_{wt}.

Here, of course, in a shale, an Archie relationship [1, pp. 57–65] between resistivity and saturation is not appropriate. Because of this in [5], the bimodal constituents are referred to as microporous (shale-like) and macroporous (sandstone-like). A good choice for independent variable is the total water saturation S_{wt} of the bimodal formation, i.e.,

$$S_{wt} = \frac{V_{sh} S_{wsh} \phi_{sh} + V_{sa} S_{wsa} \phi_{sa}}{V_{sh} \phi_{sh} + V_{sa} \phi_{sa}}. \tag{69}$$

For the purpose of plotting, define p to be

$$p^2 = \frac{(S_{wsh}\phi_{sh})^2}{(S_{wsa}\phi_{sa})^2} \tag{70}$$

then the anisotropic index κ is given by

$$\kappa = (1 + V_{sh} V_{sa} (p^2 + 1/p^2 - 2))^{1/2}. \tag{71}$$

Note from (71), the minimum value of κ is $\kappa_{\min} = 1$. In terms of the parameter p and the porosity ratio

$$\phi_r = \frac{\phi_{sh}}{\phi_{sa}} \tag{72}$$

the total water saturation S_{wt} takes the form

$$S_{wt} = S_{wsa} \frac{V_{sh} p + V_{sa}}{V_{sh} \phi_r + V_{sa}}. \tag{73}$$

Fig. 7 plots κ versus S_{wt}. The plot uses three values of fractional shale volume V_{sh} of 0.1, 0.3, and 0.5. The parameter $p = (\sigma_{sh}/\sigma_{sa})^{1/2}$ defined by (73) is used as the independent variable to generate the plot. The range of p is between $p_{\min} = 1$, resulting in a minimum value of κ, to $p_{\max}$ obtained by solving (69) for $p_{\max}$, for $\kappa = \kappa_{\max} = 20^{1/2}$. Fig. 7 uses $S_{wsa} = 0.2$ and $\phi_r = 0.1$.

IX. Conclusion

The voltage response for MWD loop antennas, located behind the drill bit in a borehole, is sensitive to the electrical anisotropy index $\kappa = (\sigma_h/\sigma_v)^{1/2}$, and the angle θ the borehole makes with respect to the axes of the anisotropy.

The index κ is a function of the water saturation S_w for finely laminated formations. Numerical results (in units of apparent resistivity) of derived analytical expressions for typical MWD array measurements show the dependence on κ, θ and S_w.

Appendix

Computation of the receiver voltage as defined by (32), from (31) and (29), depends upon the following partial derivatives:

$$\begin{aligned}
\partial^2_{xx}\Pi_x(\mathbf{x}) &= \frac{m_x k_v^2}{\kappa^2}\frac{e^{ik_v\tilde{R}}}{4\pi\tilde{R}} \\
&\quad \cdot \left[\frac{L^2\sin^2\theta}{\tilde{R}^2}\left(-1 - 3i/(k_v\tilde{R}) + 3/(k_vR)^2\right)\right. \\
&\quad \left. +1 \subset /(k_v\tilde{R}) - 1/(k_v\tilde{R})^2\right] \\
\partial^2_{xz}\Pi_x(\mathbf{x}) &= \frac{m_x k_v^2 \sin\theta\cos\theta}{\kappa^2}\frac{L^2}{\tilde{R}^2}\frac{e^{ik_v\tilde{R}}}{4\pi\tilde{R}} \\
&\quad \cdot \left[-1 - 3i/(k_v\tilde{R}) + 3/(k_v\tilde{R})^2\right] \\
\partial^2_{zz}\Pi_{z1}(\mathbf{x}) &= m_z k_h^2 \frac{e^{ik_hL}}{4\pi L} \\
&\quad \cdot \left[\cos^2\theta(-1 - 3i/(k_hL) + 3/(k_hL)^2)\right. \\
&\quad \left. +i/(k_hL) - 1/(k_hL)^2\right] \\
\partial^2_{xz}\Pi_{z1}(\mathbf{x}) &= m_z k_h^2 \sin\theta\cos\theta\frac{e^{ik_hL}}{4\pi L} \\
&\quad \cdot \left[-1 - 3i/(k_hL) + 3/(k_hL)^2\right] \\
\partial^2_{zz}\Pi_{z2}(\mathbf{x}) &= \frac{-m_x}{4\pi\kappa}\int_0^\infty J_1(\lambda\rho) \\
&\quad \cdot \left[k_{zh}^2 d^{ik_{zh}|L\cos\theta|} - k_{zv}^2 e^{ik_{zv}|L\cos\theta|}\right]\, d\lambda, \\
\partial^2_{xz}\Pi_{z2}(\mathbf{x}) &= \frac{im_x}{4\pi\kappa}\int_0^\infty \lambda\left[J_0(\lambda\rho) - \frac{J_1(\lambda\rho)}{\lambda\rho}\right] \\
&\quad \cdot \left[k_{zh} e^{ik_{zh}|L\cos\theta|} - k_{zv} e^{ik_{zv}|L\cos\theta|}\right]\, d\lambda.
\end{aligned} \tag{74}$$

In (74), without loss of generality, it is assumed that the coils are in the plane $y = 0$ and

$$\begin{aligned} \tilde{R} &= L(\sin^2\theta + \kappa^2\cos^2\theta)^{1/2} \\ m_x &= m\sin\theta \\ m_z &= m\cos\theta \\ m &= I_0 N_T A_T \\ \rho &= |L\sin\theta| \end{aligned} \tag{75}$$

where N_T is the number of turns in the transmitter coil of cross-sectional area A_T. As a check on results (74), in the limiting case when $\kappa = 1$, the medium is isotropic and the results should be independent of θ. To verify this, substitute results (74) into (32), and then (29), and (31). This gives

$$v(L,\,\theta,\,1,\,\sigma_h) = i\omega\mu_0 m_R m \frac{e^{ik_h L}}{2\pi L^3}(1 - ik_h L). \tag{76}$$

Equation (76) is well known for two-coil magnetic dipole sondes in a homogeneous and isotropic medium.

When θ approaches $\pi/2$, the numerical integrals in (74) can be highly oscillatory and difficult to evaluate. To overcome this, move the integration path into the complex plane to obtain

$$\begin{aligned} \pi_{z2}(\mathbf{x}) &= \frac{m_x}{8\pi\kappa}\int_\Gamma H_1^{(1)}(\lambda\rho) \\ &\quad\cdot\left[e^{ik_{zh}|L\cos\theta|} - e^{ik_{zv}|L\cos\theta|}\right]d\lambda \\ \partial_{zz}^2\pi_{z2}(\mathbf{x}) &= \frac{-m_x}{8\pi\kappa}\int_\Gamma H_1^{(1)}(\lambda\rho) \\ &\quad\cdot\left[k_{zh}^2 e^{ik_{zh}|L\cos\theta|} - k_{zv}^2 e^{ik_{zv}|L\cos\theta|}\right]d\lambda \\ \partial_{xz}^2\pi_{z2}(\mathbf{x}) &= \frac{im_x}{8\pi\kappa}\int_\Gamma \lambda\left[H_0^{(1)}(\lambda\rho) - \frac{H_1^{(1)}(\lambda\rho)}{\lambda\rho}\right] \\ &\quad\cdot\left[k_{zh}e^{ik_{zh}|L\cos\theta|} - k_{zv}e^{ik_{zv}|L\cos\theta|}\right]d\lambda. \end{aligned} \tag{77}$$

Results of (77) follow from properties of Hankel functions of the first kind of integer order n, $H_n^{(1)}(z)$ [8]

$$\begin{aligned} J_n(z) &= \tfrac{1}{2}\left(H_n^{(1)}(z) + H_n^{(2)}(z)\right) \\ H_n^{(2)}(-z) &= -(-1)^n H_n^{(1)}(z). \end{aligned} \tag{78}$$

Integrands in (77) are analytic in the upper λ half-plane except for branch points $\lambda = k_h$ and $\lambda = k_v$ and their associated branch cuts. The radiation condition branch cuts in the upper half-plane defined by (20) are on hyperbolic segments beginning at k_h and k_v respectively, with asymptotes on the positive imaginary λ axis. Because $H_n^{(1)}(z)$ has asymptotic behavior when $|z| \to \infty$ [8]

$$H_n^{(1)}(z) \approx \sqrt{2/(\pi z)}e^{i(z - n\pi/2 - \pi/4)}, \quad (-\pi < \arg(z) < 2\pi) \tag{79}$$

the Hankel functions in (77) have exponential convergence when $\rho > 0$. The contour Γ in integrals of (77), consists of three straight-line segments and in terms of a real parameter s is

$$\Gamma = \begin{cases} -k_m + se^{-i\phi_0}, & \text{if } s < -k_m \\ \text{real axis}, & \text{if } -k_m < s < k_m \\ k_m + se^{i\phi_0}, & \text{if } s > k_m. \end{cases} \tag{80}$$

In (80), k_m and the ray-path angle ϕ_0 are

$$\begin{aligned} k_m &= \min(\mathrm{Re}(k_h), \mathrm{Re}(k_v)) \\ \phi_0 &= \mathrm{Tan}^{-1}\left(\frac{|\mathrm{Im}(k_h - k_v)|}{|\mathrm{Re}(k_h - k_v)|}\right). \end{aligned} \tag{81}$$

Because the integrands on the first and last line segments defining path Γ in [8] decay exponentially, they are truncated when the exponent is suitably large.

ACKNOWLEDGMENT

This work originated in 1998 while the author was a Visiting Professor at Laboratório de Engenharia de Exploraço de Petróleo (LENEP), Universidade Estadual do Norte Fluminense (UENF), Macaé/RJ-Brasil. The author would like to thank the director of the laboratory, Prof. C. A. Dias, for providing the environment to make this work possible.

REFERENCES

[1] D. V. Ellis, *Well Logging for Earth Scientists*. New York: Elsevier, 1987, pp. 84–96.
[2] J. H. Moran and S. Gianzero, "Effects of formation anisotropy on resistivity-logging measurements," *Geophys.*, vol. 44, no. 7, pp. 1266–1286, 1979.
[3] J. R. Wait, *Geo-Electromagnetism*. New York: Academic, 1982.
[4] T. Hagiwara, "EM log response to anisotropic resistivity in thinly laminated formations with emphasis on 2-MHz resistivity devices," SPE Formation Evaluation, Soc. Petroleum Eng., SPE paper 28 426, 1996.
[5] J. D. Klein, P. R. Martin, and D. F. Allen, "The petrophysics of electrically anisotropic reservoirs," in *Proc. Soc. Petrol. Well-Log Analysts (SPWLA) 36th Annu. Logging Symp.*, Paris, France, June 1995.
[6] J. A. Stratton, *Electromagnetic Theory*. New York: McGraw-Hill, 1941, p. 23.
[7] C. Schlumberger, M. Schlumberger, and E. G. Leonardon, "Some observations concerning electrical measurements in anisotropic media and their interpretation," *Trans. Amer. Inst. Mining Eng. (AIME)*, vol. 110, pp. 159–182, 1934.
[8] M. Abramowitz and I. A. Stegun, *Handbook of Mathematical Functions*. Washington, DC: U.S. Govt. Printing Office, 1965.

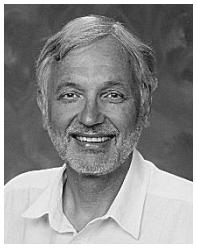

Allen Q. Howard, Jr. (M'72–SM'78–F'92) received the Ph.D. degree in physics from the University of Colorado, Boulder, in 1972, under the direction of Prof. J. R. Wait.

From 1965 to 1974, he was a Member of the Technical Staff of the Institute of Telecommunication Sciences, U.S. Department of Commerce, Boulder, CO, where he worked in terrestial radio wave propagation. In 1973, he was a Visiting Professor of Electrical Engineering at the Catholic University in Rio de Janeiro, Brazil. From 1974 to 1985, he taught in the Department of Electrical Engineering, University of Arizona, Tucson. A sabbatical year in 1982 in Glasgow, Scotland, U.K., lead to joining Schlumberger Well Services, Houston, TX. From 1993 to 1994, he was on sabbatical in the Department of Petroleum Geophysics, University of Pará, Belém, Pará, Brazil, where he directed three M.S. students and one Ph.D. student. In October 1995, he founded Terragraf, Inc., a high-resolution subsurface imaging company. He has consulted for Standard Oil, British Petroleum, Lawrence Livermore Laboratories, Los Alamos Laboratories, U.S. Department of Commerce, Schlumberger Doll Research, Sperry Sun Drilling Services, and Halliburton. His technical interests include geophysical applications of electromagnetic theory, applied mathematics, and signal processing.

Dr. Howard is a member of Commissions B and F of the International Scientific Radio Union (URSI) and SEG. He has served as Associate Editor for Electromagnetic Subsurface Remote Sensing for the IEEE TRANSACTIONS ON GEOSCIENCE AND REMOTE SENSING. In 1993, he was URSI Technical Chairman for the International Geoscience and Remote Sensing meeting.